


Molecular Tensile Machines: Intrinsic Acceleration of Disulfide Reduction by Dithiothreitol

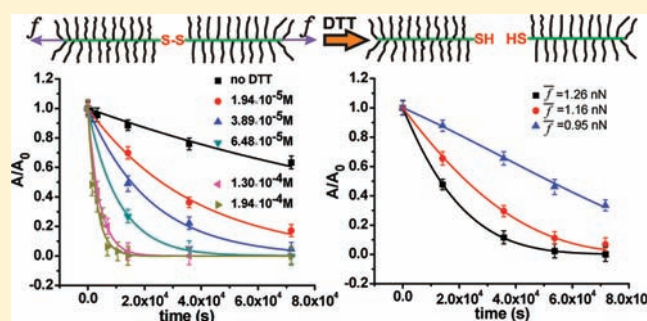
Yuanchao Li,[†] Alper Nese,[‡] Natalia V. Lebedeva,[†] Tyler Davis,[†] Krzysztof Matyjaszewski,[‡] and Sergei S. Sheiko^{*,†}

[†]Department of Chemistry, University of North Carolina at Chapel Hill, Chapel Hill, North Carolina 27599-3290, United States

[‡]Department of Chemistry, Carnegie Mellon University, 4400 Fifth Avenue, Pittsburgh, Pennsylvania 15213, United States

 Supporting Information

ABSTRACT: Significant tension on the order of 1 nN is self-generated along the backbone of bottlebrush macromolecules due to steric repulsion between densely grafted side chains. The intrinsic tension is amplified upon adsorption of bottlebrush molecules onto a substrate and increases with grafting density, side chain length, and strength of adhesion to the substrate. These molecules were employed as miniature tensile machines to study the effect of mechanical force on the kinetics of disulfide reduction by dithiothreitol (DTT). For this purpose, bottlebrush macromolecules containing a disulfide linker in the middle of the backbone were synthesized by atom transfer radical polymerization (ATRP). The scission reaction was monitored through molecular imaging by atomic force microscopy (AFM). The scission rate constant increases linearly with the concentration of DTT and exponentially with mechanical tension along the disulfide bond. Moreover, the rate constant at zero force is found to be significantly lower than the reduction rate constant in bulk solution, which suggests an acidic composition of the water surface with pH = 3.7. This work demonstrates the ability of branched macromolecules to accelerate chemical reactions at specific covalent bonds without applying an external force.



INTRODUCTION

Although the effect of mechanical forces on chemical reactions has drawn scientists' attention for centuries,^{1,2} conventional mechanochemistry remains to be largely destructive and non-selective. However, research carried out during the past several years has shown that mechanical forces can be used in a more controlled fashion through the development of special macromolecules and tools that allow management of bond tension on molecular length scales.^{1–4} These enabled scission of specific chemical bonds,^{5,6} steering of reaction pathways,⁷ changing color of materials,⁸ triggering multiple reactions in a single polymer chain,⁹ mechanocatalysis,^{10–13} reconfiguring stereoisomers,¹⁴ and controlling spin states in transition-metal complexes.¹⁵ Our contribution to this endeavor was the creation of macromolecular architectures that were able to generate bond tensions without applying an external force.^{6,16–20} Recently, we have outlined basic principles of molecular design that enable amplification, transmission, and control of tension in molecular bottlebrushes,¹⁸ pom-poms,¹⁹ and tethered macromolecules.²⁰ The bond tension in these architectures is generated due to steric repulsion between densely positioned chain-like branches (Figure 1a). Depending on the branching density and the interaction with the surrounding environment (solvent, substrate, neighboring macromolecules), the tension can be amplified from the pico-Newton to nano-Newton range, which is

sufficient to sever strong covalent bonds in single macromolecules^{6,16,17} and in dense monolayers.²¹ Here, we want to advance this concept by demonstrating the ability of branched macromolecules to accelerate chemical reactions at specific covalent bonds that are purposely inserted into a large macromolecule.

To develop a proof-of-concept, we have chosen thiol/disulfide exchange as a model reaction given its biological relevance^{22–26} and significant amount of literature.^{3,27–32} In this Article, we report the effect of inherent mechanical tension on the reduction of disulfide by dithiothreitol (DTT). The bond tension is generated by bottlebrush sections of a macromolecule and then spontaneously transmitted to a disulfide bond in the middle of the brush backbone (Figure 1a). The reduction-induced fracture of the bottlebrushes was monitored by atomic force microscopy (AFM) as a function of tension and concentration of DTT. The experimental approach based on molecular imaging is unique as it allows monitoring reactions for a large ensemble of individual macromolecules subjected to identical, yet tunable, mechanical and thermal conditions.^{33–35} This capability combines the advantages of single molecule probes and macroscopic tensile machines by offering, respectively, well-defined bond-tension distributions and representative statistics of bond-rupture events.

Received: August 16, 2011

Published: September 26, 2011

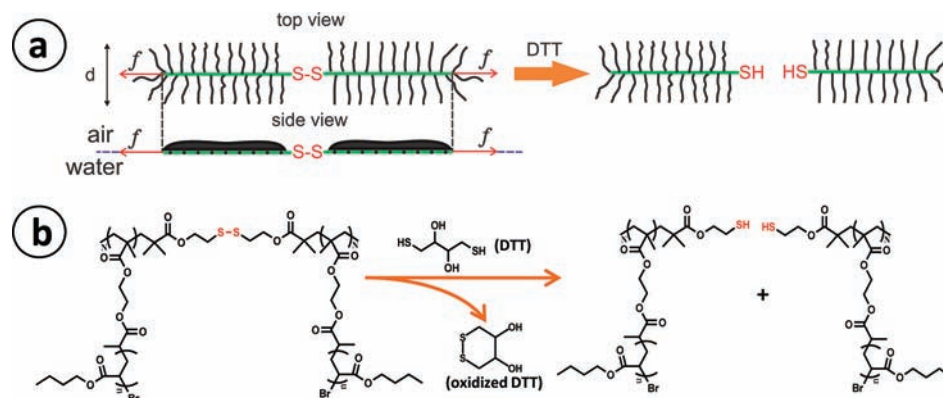


Figure 1. (a) The backbone in a bottlebrush macromolecule at the air–water interface is strained due to steric repulsion between the densely grafted side chains. The intrinsic tension in the backbone facilitates reduction of the disulfide linker with dithiothreitol (DTT). (b) Chemical structure of the studied molecular bottlebrushes with poly(*n*-butyl acrylate) side chains and a disulfide linker in the middle of the backbone.

EXPERIMENTAL SECTION

Materials. Dithiothreitol (DTT) (99%) was purchased from Acros Organics, Inc. The bottlebrush macromolecules with a disulfide bond in the middle of the backbone were synthesized by ATRP.^{6,36–39} The polymer brush consisted of a poly(2-hydroxyethyl methacrylate) backbone and poly(*n*-butyl acrylate) (PBA) side chains (Figure 1b). A combination of molecular characterization techniques (GPC, LS, gravimetric analysis, and AFM) was employed to measure the number-average degree of polymerization (DP) of the brush backbone and side chains as $2N = 1300$ and $n = 60$, respectively.⁶

Langmuir–Blodgett Monolayers. All experiments were conducted at room temperature (298 K). A small amount (50 μ L) of a dilute (0.35 mg/mL) solution of bottlebrush macromolecules in chloroform was deposited onto the surface of water/2-propanol mixtures with a certain amount of DTT in LB trough (KSV-5000 instrument equipped with a Wilhemy plate balance). Mixing water (Milli-Q double-distilled, $\rho = 18.2$ M Ω) and 2-propanol (Aldrich, 99%) allowed accurate (± 0.1 mN/m) control of the surface energy within a range of 69–72 mN/m. The measurements were performed under controlled vapor pressure of propanol to minimize the effect of solvent evaporation on the surface energy of the substrate. After different reaction times, the monolayer films were transferred from the air/water interface to mica substrates at a constant pressure of 0.5 mN/m for AFM analysis.

Atomic Force Microscopy. Topographic images of individual molecules were collected using multimode atomic force microscopy (Veeco Metrology Group) in tapping mode.³³ We used silicon cantilevers with a resonance frequency of about 160 kHz and a spring constant of about 5 N/m. The analysis of digital images was performed using a custom software program developed in-house. The length distributions were obtained from two $3 \mu\text{m} \times 3 \mu\text{m}$ AFM images, including more than 600 molecules to ensure a relative standard deviation of the mean below 4%.

RESULTS AND DISCUSSION

The obtained results are presented in two sections. First, we report the effect of DTT concentration on the rate constant of cleavage of the disulfide bond. Second, we analyze the effect of bond tension on the rate constant. Note that two reactions can occur simultaneously in the studied systems: (i) mechanically induced homolytic cleavage of the disulfide bond and (ii) mechanically accelerated reduction of the disulfide bond by DTT. Because these reactions occur on different time scales (DTT-reduction

is much faster), we conducted our experiments at lower bond tensions to suppress the homolytic cleavage and thus increase the contribution of bond scission due to reduction. It is also possible that other bonds in the backbone, such as C–C and C–S, break under tension. However, because the scission rate of C–C and C–S bonds is at least 1 order of magnitude lower than the rate of the S–S scission,⁶ the observed chain scission is ascribed to preferential cleavage of the midchain disulfide bonds. The bond tension was controlled by using molecular bottlebrushes with shorter side chains to ensure that the backbone tension is below (or just above) 1 nN.

1. The Effect of DTT Concentration. The first step in our study was to verify that DTT dissolved in the water subphase accelerates the scission of the disulfide linker in bottlebrush macromolecules adsorbed at the water/air interface. For this purpose, the kinetics of the reduction process was investigated at six different concentrations of DTT under the same tension. As an example, Figure 2 shows two AFM micrographs along with the corresponding length distributions for lower (1.94×10^{-5} M) and higher (1.94×10^{-4} M) concentrations of DTT in the water subphase. In both cases, one observed a bimodal length distribution represented by two bands at $L \cong 300$ nm and $L/2 \cong 150$ nm that correspond, respectively, to (a) the full length of bottlebrushes with the intact disulfide linker and (b) monosulfide bottlebrushes due to midchain scission of the disulfide linker during synthesis.⁶ However, the relative contribution of the intact macromolecules promptly decreases with the DTT concentration. As shown in Figure 2b, after 4 h on 1.94×10^{-4} M DTT solution substrate, the population of long molecules at $L \cong 300$ nm almost vanished, leading to the corresponding increase of the $L/2$ fraction at 150 nm. This clearly indicates that DTT promotes the scission of the disulfide linker.

Molecular imaging offers two complementary methods for quantitative analysis of the kinetics of bond scission. The first method is based on counting the number of molecules per unit area. In this case, the increasing number of molecules is equivalent to the number of ruptured bonds. The second method (used in this Article) is based on measuring the number average contour length (L) of the bottlebrush macromolecules, which decreases upon scission. Both methods are accurate; yet the first method should take into account an ill-defined variation in the molecular area (area per bottlebrush) due to separation of ruptured bottlebrushes. Therefore, we based our analysis on

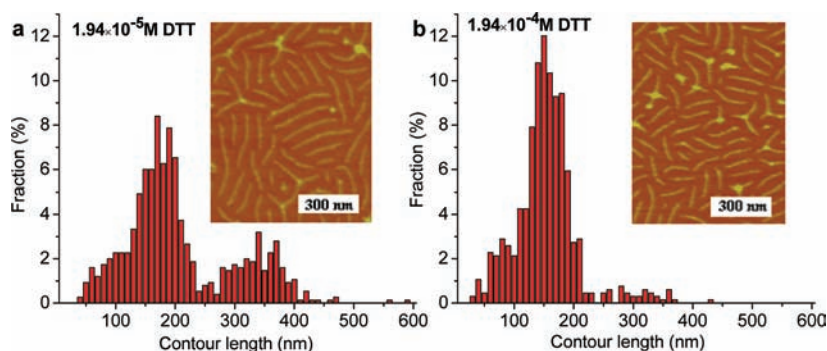


Figure 2. AFM height images along with the corresponding length distributions were measured for bottlebrush macromolecules that (prior to transfer to mica) were deposited for 4 h on water substrates containing two different concentrations of DTT: (a) 1.94×10^{-5} M and (b) 1.94×10^{-4} M.

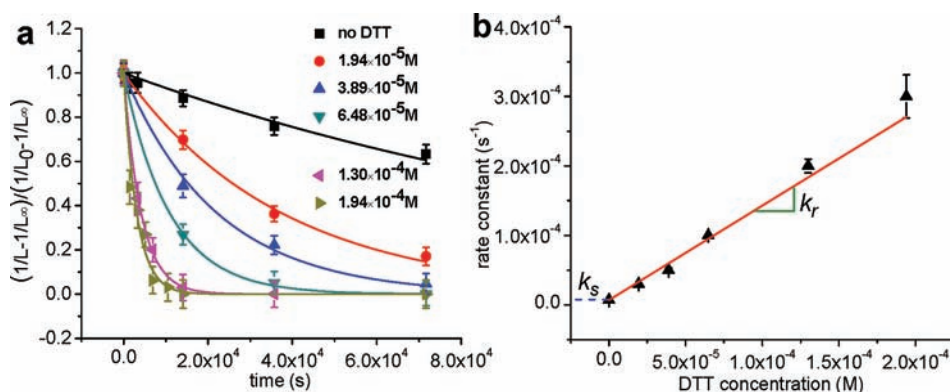


Figure 3. (a) Kinetics of the disulfide bond scission at various concentrations of DTT under the same tension ($f = 1.44$ nN). Solid lines are generated by fitting the data points with eq 1 using the rate constant k as a single fitting parameter. (b) The rate constants obtained from the fitting analysis in (a) are plotted as a function of DTT concentration. The linear fit (eq 2, solid line) gives the second-order rate constant k_r for the thiol/disulfide exchange reaction. The rate constant $k_s = 10^{-5} \text{ s}^{-1}$ at zero [DTT] was obtained from the fitting analysis of the upper set (■) of data points in (a).

monitoring the length distribution of the imaged macromolecules as a function of time. The kinetic equation is derived in Supporting Information 1 as:

$$\frac{1/L - 1/L_\infty}{1/L_0 - 1/L_\infty} = e^{-kt} \quad (1)$$

where L_0 is the initial chain length at $t = 0$ and $L_\infty = 149 \pm 3$ nm is the contour length of the midchain broken macromolecules measured long times (days, $t = \infty$). For each [DTT] data set, the initial time ($t = 0$) was assigned to the first collected data point. As mentioned above, we assume that two parallel processes contribute to the disulfide bond scission: (i) the mechanical scission of the disulfide bond (rate constant k_s) and (ii) the reduction of disulfide by DTT (rate constant k_r), which are the first- and second-order reactions, respectively. As such, the total rate constant can be written as

$$k = k_r[\text{DTT}] + k_s \quad (2)$$

Equation 1 was used to fit the experimental data points in Figure 3a using the rate constant k as a single fitting parameter. The obtained values of the rate constant were plotted as a function of DTT concentration (Figure 3b). The first data point corresponds to $k_s = 10^{-5} \text{ s}^{-1}$, that is, the rate constant at zero [DTT]. By fitting the data points in Figure 3b using eq 2, one obtains $k_r = 1.4 \text{ M}^{-1} \text{ s}^{-1}$, which is the second-order rate constant for the thiol/disulfide exchange reaction on the surface of water.

2. The Effect of Force. To study the effect of bond tension on the reduction rate constant, the bottlebrush macromolecules were deposited on the surface of different water/2-propanol mixtures. As shown previously,¹⁶ the backbone tension in adsorbed molecular bottlebrushes increases linearly with the spreading parameter S as

$$f \cong Sd(d \approx n) \quad (3)$$

where d is the width of adsorbed bottlebrushes (Figure 1a), which is proportional to the degree of polymerization of side chains (n). The spreading parameter $S = \gamma_{\text{sg}} - (\gamma_{\text{sl}} + \gamma_{\text{lg}})$ is the difference between the interfacial energies for the substrate/gas (sg), substrate/liquid (sl), and liquid/gas (lg) interfaces. In our experiments, the substrate corresponds to the water subphase, the liquid is a melt of PBA side chains, and the gas is air. On pure water at a room temperature of $T_0 = 298$ K, we measured $d = 60 \pm 2$ nm and $S = 24.0$ mN/m, which gave a backbone tension of $f_w = 1.44 \pm 0.06$ nN. Upon adding 2-propanol, the spreading parameter decreases (Figure S2 in Supporting Information 2) and so does the backbone tension (eq 3). Figure 4 presents kinetic curves measured for different values of the backbone tension at the same concentration of DTT (1.94×10^{-4} M). The figure clearly shows that an incremental increase of bond tension from 0.95 to 1.26 nN results in significant acceleration of the scission reaction.

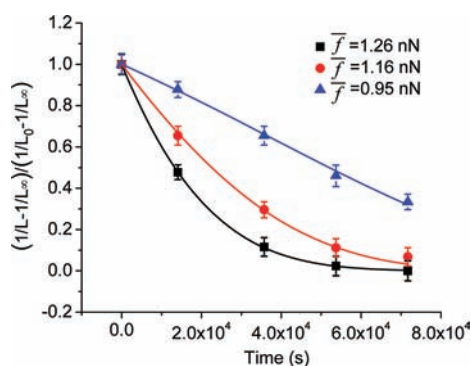


Figure 4. Kinetics of disulfide bond scission on three different substrates and, hence, backbone tensions (as indicated). The substrates were mixtures of water and 2-propanol with the following fractions of 2-propanol: 0.3% (■), 0.5% (●), and 1.0% (▲). DTT concentration was the same, 1.94×10^{-4} M, in all three experiments.

To quantify the observed tension effects, the data in Figure 4 were analyzed using a phenomenological equation proposed by Eyring, Zhurkov, and Bell for various force-activated bond-scission reactions:^{40–42}

$$k_r = k_{r,0} e^{f\Delta x/k_B T} \quad (4)$$

where $k_{r,0}$ is the rate constant at zero force, Δx is the distance from the minimum of the potential well to the transition state along the reaction coordinate,²⁹ and $k_B = 1.38 \times 10^{-23}$ J/K is Boltzmann's constant. Because the rate constant at zero force is unknown, we calculate the rate constant in eq 4 relative to the independently measured rate constant $k_{r,w}$ on a water surface as

$$k_r = k_{r,w} e^{(f - f_w)\Delta x/k_B T} \quad (5)$$

where $k_{r,w} = 1.4 \text{ M}^{-1} \text{ s}^{-1}$ and $f_w = 1.44 \text{ nN}$ (Figure 3). Here, we assume that Δx does not depend on force, which is acceptable for the narrow interval of forces studied in this Article. As mentioned in the Experimental Section, special care was taken to control the evaporation of 2-propanol and monitor the resulting variation of the spreading parameter on long time scales. Figure S3 in Supporting Information 2 shows temporal variations of the spreading parameter for the substrates studied in this Article. Within the 20 h time frame, the tension variation can be approximated with a linear equation:

$$f = at + f_0 \quad (6)$$

where a and f_0 calculated from the linear fitting results in Figure S3 are summarized in Table S1 in Supporting Information 2. Even though the effect of propanol evaporation on tension is relatively small ($\sim 20\%$ increase), the exponential $k(f)$ dependence (eq 4) requires its inclusion to the kinetics analysis. The combination of eqs 5 and 6 (eq 13 in Supporting Information 1) was used to fit the experimental data points in Figure 4 with Δx as a single fitting parameter. The determined Δx values were then used to calculate the corresponding rate constant (eq 5). Table 1 summarizes the results.

The obtained Δx values are somewhat smaller than the corresponding data from single-molecule force-clamp spectroscopy experiments^{28,29} ($\Delta x = 0.029\text{--}0.035 \text{ nm}$) and theoretical calculations ($\Delta x = 0.036 \text{ nm}$,⁴³ $\Delta x = 0.037 \text{ nm}$ ^{29,44}) conducted at contact force and using thiol-based reducing agents. There could be several reasons for this deviation. First, 3% (ca. 0.001 nm)

Table 1. Results from Fitting Analysis in Figure 4

| \bar{f}^a (nN) | Δx^b (nm) | k_r^c ($\text{M}^{-1} \text{ s}^{-1}$) |
|------------------|-------------------|--------------------------------------------|
| 1.26 | 0.024 | 0.49 |
| 1.16 | 0.026 | 0.24 |
| 0.95 | 0.029 | 0.04 |

^a $\bar{f} = at/2 + f_0$ is the average force over time. ^b Δx values were obtained from fitting analysis in Figure 4. ^c k_r was calculated using eq 5 with corresponding \bar{f} and Δx .

underestimation of the Δx value is due to the drop of bond tension in the middle section of the backbone (around the disulfide linker, Figure 1b), which does not carry side chains (Figure S4 in Supporting Information 3). Second, the covalent backbone encapsulated within a shell of tightly adsorbed side chain (Figure 1a) is significantly more constrained than polymer chains pulled by a single-molecule probe. The disulfide bond is unable to sample the entire configurational space resulting in a narrow distribution of the angle between the S–S bond and the stretching direction, which directly affects the force projection on the bond. Third, the deviation can be commonly ascribed to the intrinsic uncertainty of the scaling relation (eq 3) that predicts tension values up to a numerical coefficient of the order of unity.

We can also estimate the activation energy using the following relationship:

$$k_{r,0} = Ae^{-E_a/RT}$$

where $k_{r,0} = 1.4 \times 10^{-4} \text{ M}^{-1} \text{ s}^{-1}$ is the second-order rate constant for DTT reduction of disulfide at zero force, A is the pre-exponential factor, and R is the universal gas constant. For a broad interval of A ranging from 10^5 to $10^{12} \text{ M}^{-1} \text{ s}^{-1}$, we estimate the activation energy barrier E_a to be in the range of 51–91 kJ/mol. This is about 20 kJ/mol higher than the energy range of 30–65 kJ/mol obtained in single-molecule pulling tests at constant force,^{28,29} which may be attributed to a lower pH at the air/water interface as discussed below.

The redox rate constant depends on the pH of the reaction medium.^{45,46} Therefore, it is instructive to compare the rate constant at zero force ($k_{r,0}$) with the corresponding literature data obtained under controlled pH conditions in bulk solutions. For one of the determined Δx values, for example, $\Delta x = 0.026 \text{ nm}$, we can calculate $k_{r,0} = k_{r,w} \cdot e^{-f_w \cdot \Delta x/k_B T} = 1.4 \times 10^{-4} \text{ M}^{-1} \text{ s}^{-1}$. This value is at least 4 orders of magnitude smaller than the second-order rate constant, $5 \text{ M}^{-1} \text{ s}^{-1}$, for the DTT reduction of disulfide bonds in insulin at pH = 7.⁴⁵ Such a significant discrepancy may be due to steric inaccessibility of the disulfide bond surrounded by a shell of side chains.⁴⁷ However, in adsorbed brushes, the hydrophobic side chains are segregated at the air side of the air/water interface and, hence, do not impose significant steric constraints for small DTT molecules in the aqueous subphase. Therefore, we tentatively believe that the low rate constant is caused by a higher acidity of the surface of water with respect to the neutral bulk water.^{48–51} The pH value of the water surface can be estimated from the pH-independent rate constant $k_{r,0}^a$, which is related to the measured $k_{r,0}$ by the following equation:

$$k_{r,0}^a = k_{r,0} \cdot \frac{1 + 10^{\text{p}K_2 - \text{pH}} + 10^{\text{p}K_1 + \text{p}K_2 - 2\text{pH}}}{2 + 10^{\text{p}K_2 - \text{pH}}} \approx k_{r,0} \times 10^{\text{p}K_1 - \text{pH}} \quad (7)$$

where $pK_1 = 10.1$ and $pK_2 = 9.2$ are the first and second dissociation constants for the first and second thiols of DTT, respectively.^{46,52} From the measured $k_{r,0} = 1.4 \times 10^{-4} \text{ M}^{-1} \text{ s}^{-1}$ and the pH-independent rate constant of $k_{r,0}^a \cong 50 \text{ M}^{-1} \text{ s}^{-1}$ at a room temperature of 298 K,⁴⁶ one estimates the pH of water surface to be $\text{pH} \cong 3.7$. This value is significantly smaller than the measured $\text{pH} = 6.6$ of the bulk water/2-propanol mixture (0.5 wt/wt %). The lower pH is consistent with the recent simulation and surface-sensitive spectroscopic studies, suggesting that hydronium ion is enhanced at the air/water interface when compared to bulk solution.^{48–51} As such, our system may be used to explore the long-standing debate about the acidity of the water surface.^{53–56}

CONCLUSIONS

We have extended our studies of “molecular tensile testing machines”, bottlebrush macromolecules with a weak linker in the middle of the backbone, to probe the reduction of disulfide bonds by DTT under tension. The bond tension in the bottlebrush macromolecules is induced spontaneously without applying any external force. The kinetics of the S–S reduction process was investigated as a function of DTT concentration and backbone tension. The reduction rate was shown to linearly increase with [DTT] and exponentially increase with tension, which is in agreement with the previous literature.^{27,28,31} Although the estimated $\Delta x = 0.024\text{--}0.029 \text{ nm}$ and $E_a = 51\text{--}91 \text{ kJ/mol}$ comfortably agree with the literature data, their molecular interpretation needs to be further investigated using computational tools by taking into account the configurational constraints imposed by the bottlebrush architecture, interfacial confinement, and the aqueous environment. To summarize, our work presents a new experimental tool for quantitative studies of the force effect on chemical reactions. It provides tentative evidence that the surface of water is more acidic than bulk water. The designed “molecular tensile testing machines” may also be used to probe the chemistry of other bonds and have potential applications such as sensors, mechanocatalysts, and precursors for self-healing materials.

ASSOCIATED CONTENT

S Supporting Information. Derivation of fitting equations, time-dependence of spreading parameter, and discussion of tension drop in the middle section of the bottlebrush molecule backbone. This material is available free of charge via the Internet at <http://pubs.acs.org>.

AUTHOR INFORMATION

Corresponding Author
sergei@email.unc.edu

ACKNOWLEDGMENT

We gratefully acknowledge funding from the National Science Foundation (DMR 0906985, DMR 0969301, and CBET-0609087).

REFERENCES

- (1) Beyer, M. K.; Clausen-Schaumann, H. *Chem. Rev.* **2005**, *105*, 2921–2948.
- (2) Caruso, M. M.; Davis, D. A.; Shen, Q.; Odom, S. A.; Sottos, N. R.; White, S. R.; Moore, J. S. *Chem. Rev.* **2009**, *109*, 5755–5798.
- (3) Liang, J.; Fernández, J. M. *ACS Nano* **2009**, *3*, 1628–1645.

- (4) Huang, Z.; Boulatov, R. *Chem. Soc. Rev.* **2011**, *40*, 2359–2384.
- (5) Yang, Q.-Z.; Huang, Z.; Kucharski, T. J.; Khvostichenko, D.; Chen, J.; Boulatov, R. *Nat. Nanotechnol.* **2009**, *4*, 302–306.
- (6) Park, I.; Sheiko, S. S.; Nese, A.; Matyjaszewski, K. *Macromolecules* **2009**, *42*, 1805–1807.
- (7) Hickenboth, C. R.; Moore, J. S.; White, S. R.; Sottos, N. R.; Baudry, J.; Wilson, S. R. *Nature* **2007**, *446*, 423–427.
- (8) Davis, D. A.; Hamilton, A.; Yang, J.; Cremer, L. D.; Van Gough, D.; Potisek, S. L.; Ong, M. T.; Braun, P. V.; Martinez, T. J.; White, S. R.; Moore, J. S.; Sottos, N. R. *Nature* **2009**, *459*, 68–72.
- (9) Lenhardt, J. M.; Black, A. L.; Craig, S. L. *J. Am. Chem. Soc.* **2009**, *131*, 10818–10819.
- (10) van Leeuwen, P. W. N. M.; Kamer, P. C. J.; Reek, J. N. H.; Dierkes, P. *Chem. Rev.* **2000**, *100*, 2741–2770.
- (11) Piermattei, A.; Karthikeyan, S.; Sijbesma, R. P. *Nat. Chem.* **2009**, *1*, 133–137.
- (12) Tennyson, A. G.; Wiggins, K. M.; Bielawski, C. W. *J. Am. Chem. Soc.* **2010**, *132*, 16631–16636.
- (13) Alegre-Cebollada, J.; Perez-Jimenez, R.; Kosuri, P.; Fernandez, J. M. *J. Biol. Chem.* **2010**, *285*, 18961–18966.
- (14) Wiggins, K. M.; Hudnall, T. W.; Shen, Q.; Kryger, M. J.; Moore, J. S.; Bielawski, C. W. *J. Am. Chem. Soc.* **2010**, *132*, 3256–3257.
- (15) Parks, J. J.; Champagne, A. R.; Costi, T. A.; Shum, W. W.; Pasupathy, A. N.; Neuscammann, E.; Flores-Torres, S.; Cornaglia, P. S.; Aligia, A. A.; Balseiro, C. A.; Chan, G. K.-L.; Abruna, H. D.; Ralph, D. C. *Science* **2010**, *328*, 1370–1373.
- (16) Sheiko, S. S.; Sun, F. C.; Randall, A.; Shirvanyants, D.; Rubinstein, M.; Lee, H.-i.; Matyjaszewski, K. *Nature* **2006**, *440*, 191–194.
- (17) Lebedeva, N. V.; Sun, F. C.; Lee, H.-i.; Matyjaszewski, K.; Sheiko, S. S. *J. Am. Chem. Soc.* **2008**, *130*, 4228–4229.
- (18) Panyukov, S.; Zhulina, E. B.; Sheiko, S. S.; Randall, G. C.; Brock, J.; Rubinstein, M. *J. Phys. Chem. B* **2009**, *113*, 3750–3768.
- (19) Panyukov, S. V.; Sheiko, S. S.; Rubinstein, M. *Phys. Rev. Lett.* **2009**, *102*, 148301.
- (20) Sheiko, S. S.; Panyukov, S.; Rubinstein, M. *Macromolecules* **2011**, *44*, 4520–4529.
- (21) Park, I.; Shirvanyants, D.; Nese, A.; Matyjaszewski, K.; Rubinstein, M.; Sheiko, S. S. *J. Am. Chem. Soc.* **2010**, *132*, 12487–12491.
- (22) Chen, S.; Springer, T. A. *Proc. Natl. Acad. Sci. U.S.A.* **2001**, *98*, 950–955.
- (23) Kadokura, H.; Katzen, F.; Beckwith, J. *Annu. Rev. Biochem.* **2003**, *72*, 111–135.
- (24) Barford, D. *Curr. Opin. Struct. Biol.* **2004**, *14*, 679–686.
- (25) Yan, B.; Smith, J. W. *Biochemistry* **2001**, *40*, 8861–8867.
- (26) Mayans, O.; Wuerges, J.; Canela, S.; Gautel, M.; Wilmanns, M. *Structure* **2001**, *9*, 331–340.
- (27) Singh, R.; Whitesides, G. M. *J. Am. Chem. Soc.* **1990**, *112*, 6304–6309.
- (28) Wiita, A. P.; Ainavarapu, S. R. K.; Huang, H. H.; Fernandez, J. M. *Proc. Natl. Acad. Sci. U.S.A.* **2006**, *103*, 7222–7227.
- (29) Koti Ainavarapu, S. R.; Wiita, A. P.; Dougan, L.; Uggerud, E.; Fernandez, J. M. *J. Am. Chem. Soc.* **2008**, *130*, 6479–6487.
- (30) Kucharski, T. J.; Huang, Z.; Yang, Q.-Z.; Tian, Y.; Rubin, N. C.; Concepcion, C. D.; Boulatov, R. *Angew. Chem., Int. Ed.* **2009**, *48*, 7040–7043.
- (31) Liang, J.; Fernández, J. M. *J. Am. Chem. Soc.* **2011**, *133*, 3528–3534.
- (32) Iozzi, M. F.; Helgaker, T.; Uggerud, E. *J. Phys. Chem. A* **2011**, *115*, 2308–2315.
- (33) Sheiko, S. S.; Möller, M. *Chem. Rev.* **2001**, *101*, 4099–4124.
- (34) Sheiko, S. S.; Prokhorova, S. A.; Beers, K. L.; Matyjaszewski, K.; Potemkin, I. I.; Khokhlov, A. R.; Möller, M. *Macromolecules* **2001**, *34*, 8354–8360.
- (35) Sheiko, S. S.; Möller, M. In *Macromolecular Engineering: Precise Synthesis, Materials Properties, Applications*; Krzysztof Matyjaszewski, Y. G., Leibler, L., Eds.; Wiley: New York, 2007; Vol. 3, pp 1515–1574.
- (36) Matyjaszewski, K.; Xia, J. *Chem. Rev.* **2001**, *101*, 2921–2990.

- (37) Pakula, T.; Zhang, Y.; Matyjaszewski, K.; Lee, H.-i.; Boerner, H.; Qin, S.; Berry, G. C. *Polymer* **2006**, *47*, 7198–7206.
- (38) Sheiko, S. S.; Sumerlin, B. S.; Matyjaszewski, K. *Prog. Polym. Sci.* **2008**, *33*, 759–785.
- (39) Lee, H.-i.; Pietrasik, J.; Sheiko, S. S.; Matyjaszewski, K. *Prog. Polym. Sci.* **2010**, *35*, 24–44.
- (40) Kauzmann, W.; Eyring, H. *J. Am. Chem. Soc.* **1940**, *62*, 3113–3125.
- (41) Bell, G. *Science* **1978**, *200*, 618–627.
- (42) Zhurkov, S. N. *Int. J. Fract. Mech.* **1965**, *1*, 311–322.
- (43) Császár, P.; Csizmadia, I. G.; Viviani, W.; Loos, M.; Rivail, J.-L.; Perczel, A. *J. Mol. Struct. (THEOCHEM)* **1998**, *455*, 107–122.
- (44) Fernandes, P. A.; Ramos, M. J. *Chem.-Eur. J.* **2004**, *10*, 257–266.
- (45) Holmgren, A. *J. Biol. Chem.* **1979**, *254*, 9627–9632.
- (46) Rothwarf, D. M.; Scheraga, H. A. *Proc. Natl. Acad. Sci. U.S.A.* **1992**, *89*, 7944–7948.
- (47) Creighton, T. E. *J. Mol. Biol.* **1975**, *96*, 767–776.
- (48) Buch, V.; Milet, A.; Vácha, R.; Jungwirth, P.; Devlin, J. P. *Proc. Natl. Acad. Sci. U.S.A.* **2007**, *104*, 7342–7347.
- (49) Iuchi, S.; Chen, H.; Paesani, F.; Voth, G. A. *J. Phys. Chem. B* **2008**, *113*, 4017–4030.
- (50) Vacha, R.; Horinek, D.; Berkowitz, M. L.; Jungwirth, P. *Phys. Chem. Chem. Phys.* **2008**, *10*, 4975–4980.
- (51) Petersen, P. B.; Saykally, R. J. *J. Phys. Chem. B* **2005**, *109*, 7976–7980.
- (52) Whitesides, G. M.; Lilburn, J. E.; Szajewski, R. P. *J. Org. Chem.* **1977**, *42*, 332–338.
- (53) Beattie, J. K.; Djerdjev, A. M. *Angew. Chem.* **2004**, *116*, 3652–3655.
- (54) Beattie, J. K.; Djerdjev, A. M.; Warr, G. G. *Faraday Discuss.* **2009**, *141*, 31–39.
- (55) Creux, P.; Lachaise, J.; Graciaa, A.; Beattie, J. K.; Djerdjev, A. M. *J. Phys. Chem. B* **2009**, *113*, 14146–14150.
- (56) Mundy, C. J.; Kuo, I. F. W.; Tuckerman, M. E.; Lee, H.-S.; Tobias, D. J. *Chem. Phys. Lett.* **2009**, *481*, 2–8.